OPEN ACCESS

GAVIN PUBLISHERS

Journal of Materials Science and Research

Yadav BC, et al. J Mater Sci Res: JMSR-108.

Research Article

DOI:10.29011/ JMSR-108/100008

Sol-gel formed Grape-like Nanostructured Titania Based Liquefied Petroleum Gas Sensor

Bal Chandra Yadav*, Saroj Radheyshyam Sabhajeet, Rakesh Kumar Sonker

Department of Applied Physics, School for Physical Sciences, Nanomaterials and Sensors Research Laboratory, Babasaheb Bhimrao Ambedkar University, Lucknow, UP, India

***Corresponding author:** Bal Chandra Yadav, School for Physical Sciences, Nanomaterials and Sensors Research Laboratory, Babasaheb Bhimrao Ambedkar University, Lucknow, UP, India. Tel: + 919450094590; Email: balchandra_yadav@rediffmail.com

Citation: Yadav BC, Sabhajeet SR, Sonker RK (2018) Sol-gel formed Grape-like Nanostructured Titania Based Liquefied Petroleum Gas Sensor. J Mater Sci Res: JMSR-108. DOI:10.29011/ JMSR-108/100008

Received Date: 01 February, 2018; **Accepted Date:** 13 February, 2018; **Published Date:** 23 February, 2018

Abstract

The present work reports the preparation of Titania (TiO2) thin film by sol-gel technique and its Liquefied Petroleum Gas (LPG) sensing. TiO2 exists in numerous phases possessing different structural properties like amorphous, anatase or anatase/ rutile mixed phases. The structural analysis confirmed the formation of TiO2 having an average crystallite size 21 nm. SEM showed the regular and porous grape-like surface morphology. Band gap of the material was found as 3.65 eV. This film was employed for LPG sensing and variations in resistance with exposure of LPG was observed. Sensor response (S) as a function of time was calculated and its maximum value was found as 2.8 for 4% vol. of LPG with a response and recovery times of 240 sec and 248 secs respectively.

Keywords: Sol-gel technique ; LPG sensor; TiO_2 thin film

Introduction

Liquefied Petroleum Gas (LPG) sensor has become the interesting topic of research today in observation of fundamental research as well as industrial and domestic applications. The formation of titania is a versatile material widely used in industry, research and environmental cleaning purposes. Titanium dioxide pigment is a fine white powder when used in paints, plastics or paper, it provides for maximum whiteness and opacity. Titania exists in a number of crystalline forms, the most important of which are anatase and rutile, pure titanium dioxide does not occur in nature but is derived from ilmenite or leucoxene ores. These ores are the principal raw materials used in the manufacturing of titanium dioxide pigment. Metal oxide semiconductors are useful for the sensing of combustible gases by the change in the surface conductivity due to exposure of gases. The n-type semiconducting materials such as stannous oxide (SnO_2), zinc oxide (ZnO), titanium dioxide (TiO_2) are promising materials for gas and humidity sensors [1-9]. TiO_2 is an important metal oxide for abroad range of gas sensing applications, because of its surface chemistry, charge transport and electrical properties. It is a versatile material widely used in industry, research and environmental cleaning. Titanium dioxide is found in three different phases; rutile (tetragonal), anatase (tetragonal) and brookite (orthorhombic) and each phase has its own structure along with a particular application [10-13]. TiO_2 is a versatile functional material due to its many unusual properties such as high refractive index, hydrophilicity [13], biocompatibility [14], semi conductivity, corrosion resistance, low cost, wide availability, nontoxicity and physicochemical stable nature [15] and also known for its gas sensing behavior [16,17]. Titanium dioxide has received considerable attention because of its excellent optical, electrical, mechanical, and catalytic properties, which makes it technologically useful. Its superior properties are due to chemical and biological inertness, non-toxicity, strong oxidising/reducing power, cost-effectiveness and long-term stability against photo-corrosion and chemical corrosion. The band gap of titania is about 3.2 eV. The band gap further increases with decreasing the particle size and hence the utilisation typically confined within the UV-radiation of the electromagnetic spectrum. The basic requirement for the sensor is the change in electrical conductivity with exposure of LPG to the surface of semiconducting oxides which depends on their band gaps, surface morphology, size, the diffusion rate of gas and specific surface area. The semi-conducting properties of metal oxides represent the basis for their use as gas sensors, since the number of free charge carriers within the metal oxide and thus its

electrical conductivity reversibly depends on the interactions with the ambient gas atmosphere.

Since the LPG sensing mechanism is based on the chemisorptions reaction that takes place at the surface of the metal oxide. Thus, increasing specific surface area of the sensing film leads to more sites for the adsorption of surrounding gases. The oxygen adsorbed on the surface of the film influences the resistance of the titania based sensor. Initially oxygen from the atmosphere adsorbs on the surface of the film and extracts electrons from its conduction bands to form O_2^- species on the surface, consequently resistance decreases. After that, an equilibrium state is achieved between the oxygen of TiO_2 and atmospheric oxygen.

Materials and Methods

Titanium tetrachloride ($TiCl_4$), propanol, deionizer water (DI) and ethanol wereused for the material preparation. All chemicals were purchased from Sigma-Aldrich Chemical Co. with 99.99% purity.

Synthesis of Material

50 ml of $TiCl_4$ aqueous solution was added dropwise to 250 ml of ice-water at room temperature under vigorous stirring to obtain dilute $TiCl_4$ aqueous solution. Then 40 g of citric acid was added to it which made it a transparent solution. After annealing at 250 ºC for 24 h, TiO_2in powder form was obtained [18].

Thin Film Deposition Technique

Spin coating is a method which is generally employed for the preparation of thin films. A typical process involves depositing a small puddle of a fluid material onto the centre of a substrate and then spinning the substrate at high speed. Centripetal acceleration will cause most of the resin to spread to, and eventually off, the edge of the substrate leaving a thin film of the material on the surface. Final film thickness and other properties will depend on the nature of the fluid material (viscosity, drying rate, surface tension, etc.) and the parameters chosen for the spin process. Factors such as final rotation speed, acceleration, and fume exhaust affect the properties of the coated films. Spin speed is one of the most important factors in spin coating. The speed of the substrate (rpm) affects the degree of radial (centrifugal) force applied to the fluid resin as well as the velocity and characteristic turbulence of the air immediately above it [19].

A thin film of the sample was prepared by spin coating method. For this purpose, the synthesised powder was dissolved in isopropyl alcohol and was then sonicated for 30-40 min. The sonicated solution was stirred at 100˚C for 6 h. Then a drop of the obtained solution was spun on the well-cleaned borosilicate glass substrate using spin coater (METREX SCIENTIFIC INSTRUMENTS). The resulting thin film was dried at 120˚C for 10 min for each time of deposition [9]. this drying procedure stabilises the thin film. Further, the film was annealed at 300˚C which converts the anatase phase into rutile with almost uniform and porous structure [20]. The thickness of the film was found 0.4 μm, measured by Accurion variable angle spectroscopic ellipsometer (Nanofilm EP3 Imaging). Further, two electrodes were fabricated on opposite end of the film with the silver paste for signal registration. Variations in resistance with the variation in concentration of LPG were recorded using Keithley Electrometer [6517 B].

Characterization of TiO_2

Scanning Electron Microscopy (SEM)

(Figures 1(a) and 1(b)) show SEM images of TiO_2 thin film at micro scale and nano scale, respectively. The SEM image at the micro scale shows that some of the particles combined with each other to form clusters and leaving some spaces as pores. The uniformly distributed pores with random size may also be seen through SEM image at the nanoscale. These pores serve as gas adsorption sites and gas sensitivity depends on their depths and sizes. The gas response of sensors is mainly due to the interactions between target gas and the surface of the sensor. Therefore, it is obvious that for the greater specific surface area for adsorption of LPG, the interactions between the adsorbed gases and the sensor surface would be stronger, as a result, the sensor response will be higher. In the present investigation, the improved sensing performance of sample may be attributed to their porous spherical structure and crystallite size. The pores in irregular nanospheres can act as channels for diffusion of LPG and thus provide more active sites where LPG molecules get absorbed and counter the surface species (O_2, O_2^-, O^-). This improves the reaction of LPG with surface adsorbed oxygen and is an imperative parameter regarding the sensitivity of the sensor. A close look of micrograph gives the average pore size as 100 nm which may contain many in-situ mesopores. The Specific Surface Area (SSA) was determined using the equation [6].

$$S = \frac{6}{d \times D_m} \qquad (1)$$

Where d is the bulk density of titania pellet and D_m is the average crystallite size. The number 6 is the shape factor. The specific surface area of titania pellet is 621.1 m^2/g. The high value of the active surface area is another significant feature for gas sensing.

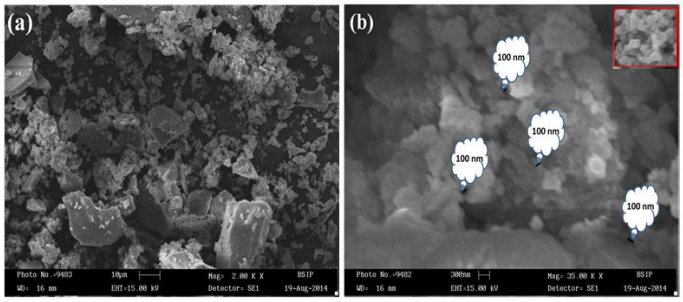

Figures 1(a-b): SEM image of TiO_2 thin film at (a) microscale (b) nanoscale.

X-Ray Diffraction

X-Ray diffraction pattern of as-prepared material shown in Figure 2 reveals the anatase phase. The average crystallite size (D) of the sensing material can be calculated by the Debye-Scherer's formula, which is given by [21].

$$D = \frac{K\lambda}{\beta cos\theta} \qquad (2)$$

where K = 0.94 is Scherer's coefficient, which depends on the shape of the crystallite and the type of defects present, λ is the wavelength of X-ray radiation, β is the full width at half maximum (FWHM) of the diffraction peak and θ is the angle of diffraction.

The XRD pattern of TiO_2 thin film also reveals that the sensing material consists of peaks. It may be observed that from (Figure 2), the peaks observed at 2θ = 25.29º, 38.49º, 48.59º, 54.73ºand 55.86º correspond to (110), (101), (200), (105) and (211) reflection planes of TiO_2, respectively and are in good agreement with the corresponding values reported for the anatase structure of TiO_2. The average crystallite size of TiO_2 thin film was calculated as ~21 nm by Debye-Scherer's formula [21]. The reduced crystallite size provides a large surface to volume ratio, hence the ability for adsorption of gas through the pores on the surface of the thin film increases which enhances the sensitivity of the gas sensor.

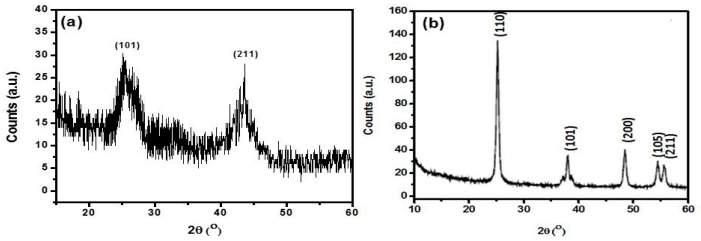

Figure 2: X-Ray Diffraction of synthesised TiO_2 thin film (a) as prepared (b) annealed at 400°C.

UV-Visible Spectroscopy

The optical transmission spectra of the as-grown TiO_2 thin film (200 nm) deposited separately on the glass substrate was investigated in the wavelength range of 190 to 1100 nm, and the variation is shown in (Figure 3). TiO_2 thin film exhibits a high transmission (>75%) in the visible region and shows a sharp fundamental absorption edge in UV region at 380 nm.

It is known that the properties of optical absorption are relevant to the electronic structure and hence are the key factor in determining the band gap. The optical energy band gap was calculated by Tauc relation as given [9].

$$\alpha h\nu = A(h\nu - E_g)^{\frac{1}{2}} \qquad (3)$$

Where A is a constant, $h\nu$ is the photon energy, E_g is the energy band gap and α is the absorption coefficient given by:

$$\alpha = 2.303 \left(\frac{A_b}{t}\right) \qquad (4)$$

In (Equation 4), A_b is the absorbance and t is the thickness of the film. Optical band gap of the TiO_2 thin film deposited on the glass substrate was calculated from the intercept on energy axis obtained by extrapolating the linear portion of the Tauc plot i.e. $(\alpha h\nu)^2$ *vs* photon energy ($h\nu$) as shown inset of (Figure 3). Estimated value of band gap for as-grown TiO_2 thin film is found to be 3.65 eV and is close to the actual values for TiO_2 thin films (3.2 eV) grown by various other techniques.

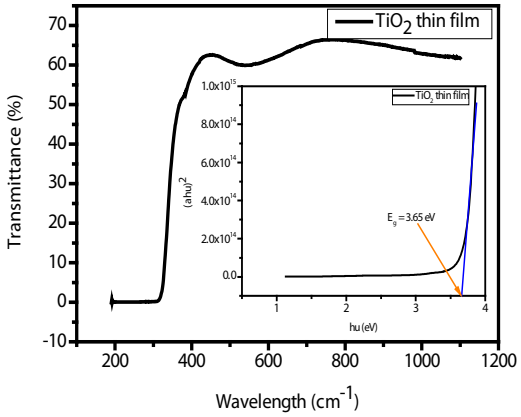

Figure 3: Transmittance spectra of TiO_2 thin film and Tauc plot; $(\alpha h\nu)^2$ versus $h\nu$.

Gas Sensing Measurements

The schematic diagram of LPG sensing set-up is shown in (Figure 4 (a)). The sensing film was inserted between the silver electrodes inside the glass chamber having two knobs. One knob is associated with the concentration measuring system (gas inlet) and other is an outlet knob for releasing the gas [22]. Concentration measuring system is shown in (Figure 4 (b)), which consists of a glass bottle containing double distilled water, which is saturated

with LPG, in order to avoid the possibility of dissolution of inserted gas. At the top of the bottle, the measuring tube (pipette) is connected by a vacuum seal. The cock I is connected to the LPG cylinder and cock II is connected to the inlet of the gas chamber. When the cock I is opened, the LPG from the cylinder is filled in the glass bottle and an equivalent amount of water is displaced in the measuring pipette. When the cock II is opened, the desired amount of gas (Equations 1, 2, 3, 4) vol.% and onwards entered in the gas chamber [23]. Before passing the LPG into chamber, the gas chamber with a resistance measuring holder was stabilised for 10-20 minutes. A sensing film with silver contacts was used for measurements of LPG sensing properties. The resistance of the film was taken as the stabilised resistance in the presence of air (R_a). When LPG was introduced to the chamber, the variations in electrical resistance with time for different vol.% of LPG were recorded by using Keithley electrometer (Model: 6517 B).

Sensitivity of the LPG sensor is defined as the change in resistance in the presence of gas (R_g) to the resistance in the presence of air (R_a), that is;

$$S = \frac{R_a}{R_g} \qquad (5)$$

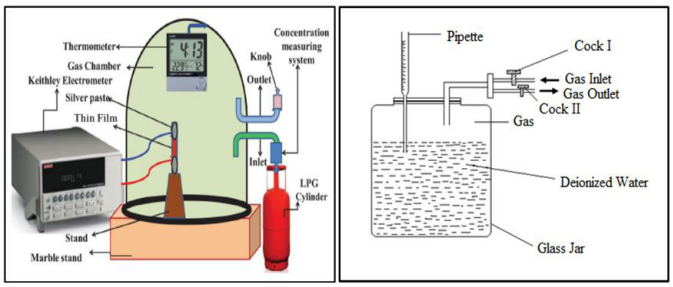

Figures 4(a-b): (a) Gas sensing set-up; Lab Model (b) Concentration measuring system.

Gas Sensing Behaviour of Metal Oxide

From the band theory for applied sensor, the target gas interacts with the surface of a metal oxide film (through the absorbed oxygen ion by surface) which results in change in charge carrier concentration of the material [24]. This change in charge carrier concentration alters the conductivity of material. An n-type semiconductor is one where the majority charge carriers are electrons and on interaction with a reducing gas an increase in conductivity (or decrease in resistance) occurs. Conversely, an oxidising gas serves to deplete the sensing layer of charge carrying the electrons resulting in a decrease in conductivity. A p-type semiconductor is a material that conducts with holes being the majority charge carriers; hence the opposite effects are observed with the material and show an increase in conductivity in the presence of an oxidising gas. A summary of response is given as below [25].

Classification of material	Reducing gas	Oxidizing gas
n-type	Resistance decrease	Resistance increase
p-type	Resistance increase	Resistance decrease

Gas sensing behaviour of TiO_2 thin film

(Figure 5) illustrates the variations in resistance of the TiO_2 film with time after exposure for different vol.% of LPG at room temperature. The curve for 1 vol.% of LPG shows the slow decrease in resistance with time after exposure of the gas. Curves for 2 & 3 vol.% of LPG exhibit the improved response and has better sensitivity than 1 vol.%. Further, for 4 vol.% of LPG resistance decreases sharply with time after exposure up to 1000 s and then become constant. The sensing response of different vol.% concentration with response and recovery times is depicted in (Table 1).

Classification of material	1 vol%	2 vol%	3 vol%	4 vol%
Response	1.73	1.65	2.52	2.80
Response Time (min)	5.21	10	3.31	4
Recovery Time (min)	8.15	13	4.43	4.13

Table 1: Sensing response of different vol.% concentration.

(Figure 6) exhibits the variations of average sensitivity with the concentration of LPG and it was found that as the concentration of LPG (in vol.%) increases, the average sensor response increases linearly up to 4 vol.% of LPG. The linear increment of the sensitivity of the sensor is a significant factor for the device fabrication. It's maximum value was obtained as ~0.65 for 4 vol.% of LPG.

The gas sensing mechanism of TiO_2 thin film-based sensor belongs to surface control type, i.e. resistance change is controlled by the contact surface area and the amount of chemisorbed oxygen. LPG consists of CH_4, C_3H_8, and some hydrocarbons. In each composition, the reducing hydrogen species are bound to a carbon atom, therefore, LPG dissociates into the reactive reducing components hardly on the surface of the sensing element. As LPG is exposed to sensing element, the conductivity increases due to the adsorption of oxide and capture more electrons that reduce the current. It was observed that as the concentration of LPG increases, the average sensitivity increases linearly in the beginning and later it becomes saturated. The linear relationship between sensitivity and gas concentration may be attributed to the availability of a sufficient number of sensing sites on the film to act upon the LPG. The low concentration implies a lower surface coverage of gas molecules, resulting in a lower surface reaction between the surface adsorbed oxygen species and the gas molecules. The increase in

LPG concentration increases the surface reaction due to a large surface coverage. Further, an increase in the LPG concentration does not increase the surface reaction and eventually saturation takes place.

Thus, the maximum sensor response was obtained at higher concentration of LPG i.e. 4 vol.%. The linearity of average response for the LPG suggests that the screen-printed TiO_2 nanocomposite film can be reliably used to monitor the LPG over this range of concentration. As the Lower Explosive Limit (LEL) for LPG is 5.0 vol. %, therefore, response is measured up to 4.0 vol. % in order to detect the LPG below LEL for safety requirement [26].

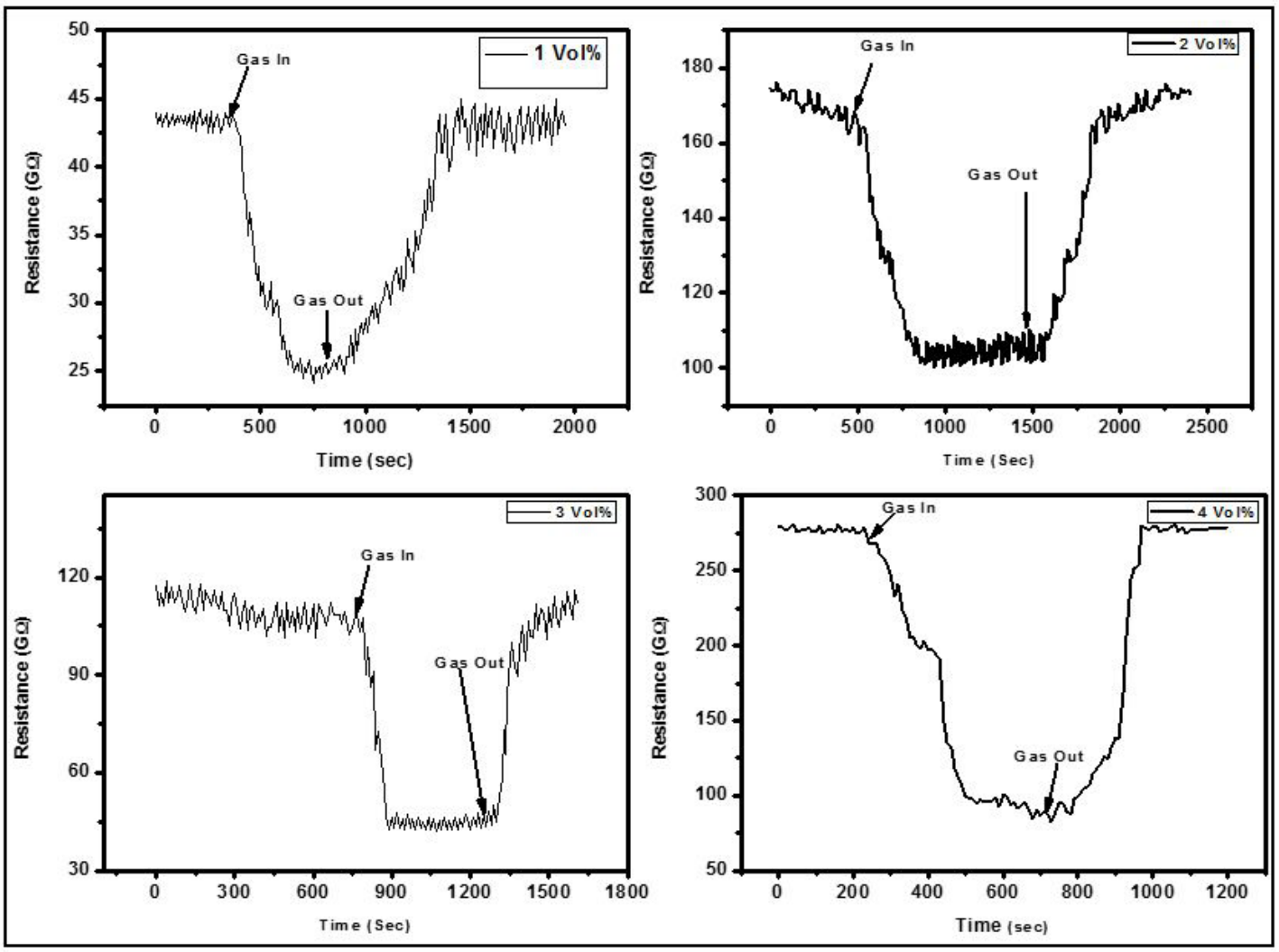

Figure 5: Variations in resistance of TiO_2 thin film with time after exposure for different Vol. % of LPG.

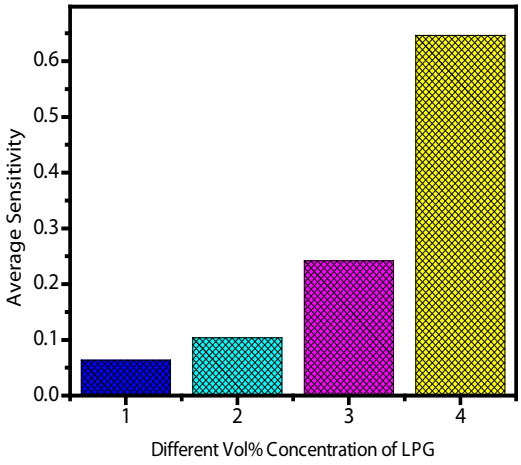

Figure 6: Variations of average sensor response of TiO_2 thin film with different concentrations of LPG.

Sensing Mechanism

The oxygen adsorbed on the surface of the film affects the resistance of the titania based sensor. Initially oxygen from the atmosphere get adsorbed on the surface of the film and extracts electrons from its conduction bands to form O_2^- species on the surface, after that, an equilibrium state is achieved between the lattice oxygen of TiO_2 and atmospheric oxygen and further the value is stabilized.

$O_2(\text{gas}) \leftrightarrow O_2(\text{ads})$ (Thin Film Surface) (6)

$O_2(\text{gas}) + e^- e^- \leftrightarrow O_2^- O_2^-$ (Thin Film Surface) (7)

When the thin film is being exposed to LPG, it reacts with the chemisorbed oxygen. On interaction with hydrocarbons (C_nH_{2n+2}) of LPG, the adsorbed oxygen is removed, forming gaseous species and water vapour. Consequently, the resistance changes, which is due to the change in the width of depletion layer after exposure to LPG. The overall reaction of LPG with the chemisorbed oxygen may take place as shown below [27].

$$C_4H_{10} + 13O^- \rightarrow 4CO_2 + 5H_2O + 13\,e^- \quad (8)$$

$$C_4H_{10} + \tfrac{13}{2} O_2^- \rightarrow 4CO_2 + 5H_2O + \tfrac{13}{2} e^- \quad (9)$$

$$C_4H_{10} + 13O^{2-} \rightarrow 4CO_2 + 5H_2O + 26\,e^- \quad (10)$$

$$C_3H_8 + 10\,O^- \rightarrow 3CO_2 + 4H_2O + 10\,e^- \quad (11)$$

$$C_3H_8 + 5\,O_2^- \rightarrow 3CO_2 + 4H_2O + 10\,e^- \quad (12)$$

$$C_3H_8 + 10\,O^{2-} \rightarrow 3CO_2 + 4H_2O + 20\,e^- \quad (13)$$

It is evident from the proposed reaction schemes that a large number of electrons are released upon LPG exposure to TiO_2 surface; particularly in the presence of O_2^- which is responsible for the rapid increase in conductivity. Recovery process of sensor is based on the desorption mechanism of LPG. The improvement in the performance of the sensor towards reducing gases has been reported in (Table 2) and can be explained by 'spill over' mechanism of oxygen atoms from the TiO_2 surface [28-32].

Sensing materials	Method of preparation	Doping /catalyst	Gas conc.	Temp. (°C)	Response (%)	Res. time (s)	Rec. time (s)	Ref. no.
TiO_2 thin film	CBD	p-poly aniline	0.1vol.%	RT	63%	440	180	Lee et al. 2002 [28]
TiO_2 thick film	CBD	Poly -pyrrol	260-1040 ppm	RT	55%	112	131	Chakraborty et al. 2006 [29]
TiO_2 thin film	Spray pyrolysis technique	Ni	1000 ppm	250	90%	300	600	Satyanarayana et al. 2003 [30]
TiO_2nanowires	Hydrothermal technique	–	500 ppm	400	3.91	25	–	Le et al. 2009 [31]
TiO_2 thin film	–	Nb	–	–	18	4000	790	Bulakhe et al. 2013 [32]
TiO_2 thin film	Chemical Route	-	4 vol.%	RT	2.8	240	248	Present Work

Table 2: Summary of result for LPG sensor based on TiO_2 thin film.

Conclusions

In this work, LPG sensor operable at room temperature was fabricated using titanium oxide thin film prepared by sol-gel route successfully. Film thickness was measured as 0.4 µm and average crystallite size was estimated at 21 nm. The maximum sensing response as ~ 2.8 was achieved for 4 vol.% of LPG with a response and recovery times of 240 sec and 248 secs respectively. This sensor structure may be exploited for the device fabrication for the detection of LPG below LEL. Also, by using appropriate do pants, the band-gap of synthesised material can be engineered so that the sensitivity of the sensor may enhance.

References

1. Patil DR, Patil LA (2007) Room temperature chlorine gas sensing using surface modified ZnO thick film resistors. Sens Actuators B Chem123: 546-553.
2. Cretu V, Postica V, Mishra A K, Hoppe M, Tiginyanu I, et al. (2016) Synthesis, characterization and DFT studies of zinc-doped copper oxide nanocrystals for gas sensing applications. Journal of Materials Chemistry A 4: 6527-6539.
3. More AM, Gunjakar JL, Lokhande CD (2008) Liquefied petroleum gas (LPG) sensor properties of interconnected web-like structured sprayed TiO_2 films. Sens Actuators B Chem 129: 671-677.
4. Sonker RK, Sharma A, Tomar M, Gupta V, Yadav BC (2014) Nanocatalyst (Pt, Ag and CuO) Doped SnO_2 Thin Film Based Sensors for Low Temperature Detection of NO_2 Gas. Adv Sci Lett 20: 1374-1377.
5. Sonker RK, Sabhajeet SR, Singh S, Yadav BC (2015) Synthesis of ZnO nanopetals and its application as NO_2 gas sensor. Materials Letters 152: 189-91.
6. Sonker RK, Yadav BC (2015) Growth mechanism of hexagonal ZnO nanocrystals and their sensing application. Materials Letters 160: 581-584.
7. Sonker RK, Sharma A, Tomar M, Gupta V, Yadav BC (2014) Low Temperature Operated NO_2 Gas Sensor Based on SnO_2-ZnO Nanocomposite Thin Film. Adv Sci Lett 20: 911-916.
8. Enachi M, Lupan O, Braniste T, Sarua A, Chow L, et al. (2015) Integration of individual TiO_2 nanotube on the chip: Nanodevice for hydrogen sensing. Phys Status Solidi RRL: 1-4.
9. Sonker RK, Sabhajeet SR, Yadav BC (2016) TiO_2-PANI nanocomposite thin film prepared by spin coating technique working as room temperature CO2 gas sensing. J Mater Sci Mater Electron 27: 11726-11732.
10. Xiabo C, Mao SS (2007) Titanium dioxide nanomaterials: synthesis, properties, modifications, and applications. Chem Rev 107: 2891-2906.
11. Fujishima A, Honda K (1972) Electrochemical photolysis of water at a semiconductor electrode. Nature 238: 37-38.
12. Diebold U (2003) The surface science of titanium dioxide. Surf Sci Rep 48: 53-229.
13. Carp O, Huisman CL, Reller A (2004) Photoinduced Reactivity of Titanium Dioxide. Prog Solid State Chem 32: 33-177.
14. Jho AK, Prasad K, Kulkarni AR 2009 Synthesis of TiO_2 nanoparticles using microorganisms. Colloids Surf 71: 226-229.
15. Kwon CH, Shin H, Kim JH, Choi W S, Yoon KH (2004) Degradation of methylene blue via photo catalysis of titanium dioxide. Mater Chem Phys 86: 78-82.
16. Skubal LR, Meshkov NM, Vogt MC (2002) Detection and identification of gaseous organics using a TiO_2 sensor. J Photochem Photobiol 148: 103-108.
17. Meier KR, Gratzel M (2002) Redox Targeting of Oligonucleotides Anchored to Nanocrystalline TiO_2 Films for DNA Detection. Chem Phys Chem 3: 371-374.
18. Yadav BC, Verma N, Singh S (2012) Nanocrystalline SnO_2-TiO_2 thin film deposited on base of equilateral prism as an opto-electronic humidity sensor. Optics & Laser Technology 44: 1681-1688.
19. Sonker RK, Yadav BC, Sharma A, Tomar M, Gupta V (2016) Experimental investigations on NO_2 sensing of pure ZnO and PANI-ZnO composite thin films. RSC Advances 6: 56149-56158.
20. Yadav BC, Shukla RK, Bali LM (2005) Sol-gel processed TiO_2 films on U-shaped glass-rods as optical humidity sensor. Indian Journal of Pure and Applied Physics 43: 51-55.
21. Sonker RK, Yadav BC (2016) Low temperature study of nanostructured Fe_2O_3 thin films as NO_2 sensor. Materials Today Proceedings 3: 2315-2320.
22. Srivastava R, Yadav BC (2015) Nanostructured $ZnFe_2O_4$ thick film as room temperature liquefied petroleum gas sensor. J ExpNanosci 10: 703-717.
23. Yadav B C, Srivastava R, Yadav A, Srivastava V (2008) LPG Sensing of Nanostructured Zinc Oxide and Zinc Niobate. Sens Lett 6: 714-718.
24. Fine GF, Cavanagh LM, Afonja A, Binions R (2010) Metal Oxide Semi-Conductor Gas Sensors in Environmental Monitoring. Sensors 10: 5469-5502.
25. William DE (1999) Semiconducting oxides as gas-sensitive resistors. Sens Actuators B Chem 57: 1-16.
26. Yadav BC, Yadav A, Shukla T, Singh S (2009) Experimental investigations on solid state conductivity of cobaltzincate nanocomposite for liquefied petroleum gas sensing. Sens Lett 7: 1119-1123.
27. Sonker RK, Yadav B C (2014) Chemical route deposited SnO_2, SnO_2-Pt and SnO_2-Pd thin films for LPG detection. Adv Sci Lett 20: 1023-1027.
28. Lee DS, Lee DD, Ban SW, Lee M, Kim YT (2002) SnO_2 Gas Sensing Array for Combustible and Explosive Gas Leakage Recognition. IEEE Sensors Journal 2: 140-149.
29. Chakraborty S, Sen A, Maiti H S (2006) Selective detection of methane and butane by temperature modulation in iron doped tin oxide sensors. Sens Actuators B Chem 115 :610-613.
30. Satyanarayana L, Reddy KM, Manorama SV (2003) Synthesis of nanocrystalline $Ni1- xCoxMnxFe_2- xO_4$: a material for liquefied petroleum gas sensing. Sens Actuators B Chem 89: 62-67.
31. Le DTT, Vuong DD, Chien ND (2009) Synthesis and LPG-sensing properties of TiO_2 nanowires. J of Physics Conference Series 187: 012086.
32. Bulakhe RN, Patil SV, Deshmukh PR, Shinde NM, Lokhande CD (2013) Fabrication and performance of polypyrrole (Ppy)/TiO_2 heterojunction for room temperature operated LPG sensor. Sens Actuators